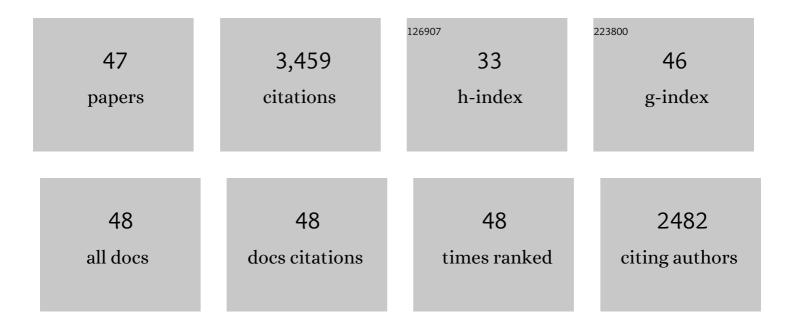
Catherine Mevel

List of Publications by Year in descending order

Source: https://exaly.com/author-pdf/3561300/publications.pdf Version: 2024-02-01



#	Article	IF	CITATIONS
1	Serpentinization of abyssal peridotites at mid-ocean ridges. Comptes Rendus - Geoscience, 2003, 335, 825-852.	1.2	363
2	Thin crust, ultramafic exposures, and rugged faulting patterns at the Mid-Atlantic Ridge (22°–24°N). Geology, 1995, 23, 49.	4.4	324
3	Constraints on deformation conditions and the origin of oceanic detachments: The Mid-Atlantic Ridge core complex at 15°45′N. Geochemistry, Geophysics, Geosystems, 2003, 4, .	2.5	234
4	Dynamic control on serpentine crystallization in veins: Constraints on hydration processes in oceanic peridotites. Geochemistry, Geophysics, Geosystems, 2007, 8, n/a-n/a.	2.5	187
5	Tectonic setting and mineralogical and geochemical zonation in the Snake Pit sulfide deposit (Mid-Atlantic Ridge at 23 degrees N). Economic Geology, 1993, 88, 2018-2036.	3.8	172
6	Hydrothermal activity along the southwest Indian ridge. Nature, 1998, 395, 490-493.	27.8	146
7	Emplacement of deep crustal and mantle rocks on the west median valley wall of the MARK area (MAR,) Tj ETQq1	1_0,78431 2.2	14 rgBT /Ov 128
8	Characteristics and evolution of the segmentation of the Mid-Atlantic Ridge between 20°N and 24°N during the last 10 million years. Earth and Planetary Science Letters, 1995, 129, 55-71.	4.4	125
9	Direct observation of a section through slow-spreading oceanic crust. Nature, 1989, 337, 726-729.	27.8	124
10	Helium and methane measurements in hydrothermal fluids from the mid-Atlantic ridge: The Snake Pit site at 23°N. Earth and Planetary Science Letters, 1991, 106, 17-28.	4.4	109
11	Isotopic portrayal of the Earth's upper mantle flow field. Nature, 2007, 447, 1069-1074.	27.8	104
12	A discontinuity in mantle composition beneath the southwest Indian ridge. Nature, 2003, 421, 731-733.	27.8	98
13	Chlorine isotopic composition in seafloor serpentinites and high-pressure metaperidotites. Insights into oceanic serpentinization and subduction processes. Geochimica Et Cosmochimica Acta, 2008, 72, 126-139.	3.9	97
14	Tectonic structure, evolution, and the nature of oceanic core complexes and their detachment fault zones (13°20′N and 13°30′N, Mid Atlantic Ridge). Geochemistry, Geophysics, Geosystems, 2017, 18, 14.	51-1482.	94
15	Zircon Dating of Oceanic Crustal Accretion. Science, 2009, 323, 1048-1050.	12.6	88
16	Amphibolite facies conditions in the oceanic crust: example of amphibolitized flaser-gabbro and amphibolites from the Chenaillet ophiolite massif (Hautes Alpes, France). Earth and Planetary Science Letters, 1978, 39, 98-108.	4.4	73
17	Additional 40Ar-39Ar dating of the basement and the alkaline volcanism of Gorringe Bank (Atlantic) Tj ETQq1 1 0.	784314 rg 4.4	gBT /Overloo 73
18	FUJI Dome: A large detachment fault near 64°E on the very slow-spreading southwest Indian Ridge. Geochemistry, Geophysics, Geosystems, 2003, 4, .	2.5	60

CATHERINE MEVEL

#	Article	IF	CITATIONS
19	Amphibolitized sheared gabbros from ophiolites as indicators of the evolution of the oceanic crust: Bay of Islands, Newfoundland. Earth and Planetary Science Letters, 1982, 61, 151-165.	4.4	59
20	Metamorphism in oceanic layer 3, Gorringe Bank, eastern Atlantic. Contributions To Mineralogy and Petrology, 1988, 100, 496-509.	3.1	56
21	An example of a recent accretion on the Mid-Atlantic Ridge: the Snake Pit neovolcanic ridge (MARK) Tj ETQq1 1 (0.784314 2.2	rgBT /Overloc
22	Metasomatic hydrous fluids in amphibole peridotites from Zabargad Island (Red Sea). Earth and Planetary Science Letters, 1993, 120, 187-205.	4.4	48
23	Evolution of oceanic gabbros from DSDP Leg 82: influence of the fluid phase on metamorphic crystallizations. Earth and Planetary Science Letters, 1987, 83, 67-79.	4.4	44
24	Magnetic signatures of serpentinization at ophiolite complexes. Geochemistry, Geophysics, Geosystems, 2016, 17, 2969-2986.	2.5	44
25	The geodynamic evolution of the South-Tethyan, margin in Zanskar, NW-Himalaya, as revealed by the Spongtang ophiolitic melanges. Geodinamica Acta, 1987, 1, 283-296.	2.2	44
26	Stretching of the deep crust at the slow-spreading Southwest Indian Ridge. Tectonophysics, 1991, 190, 73-94.	2.2	42
27	Clinopyroxenes in Mesozoic pillow lavas from the French Alps: influence of cooling rate on compositional trends. Earth and Planetary Science Letters, 1976, 32, 158-164.	4.4	41
28	Occurrence of pumpellyite in hydrothermally altered basalts from the Vema fracture zone (mid-Atlantic ridge). Contributions To Mineralogy and Petrology, 1981, 76, 386-393.	3.1	40
29	TOBI sidescan sonar imagery of the very slow-spreading Southwest Indian Ridge: evidence for along-axis magma distribution. Earth and Planetary Science Letters, 2002, 199, 81-95.	4.4	40
30	Observation of sections of oceanic crust and mantle cropping out on the southern wall of Kane FZ (N. Atlantic). Terra Nova, 1994, 6, 143-148.	2.1	39
31	A geological cross-section of the Vema fracture zone transverse ridge, Atlantic ocean. Journal of Geodynamics, 1991, 13, 97-117.	1.6	37
32	Chromian jadeite, phengite, pumpellyite, and lawsonite in a high–pressure metamorphosed gabbro from the French Alps. Mineralogical Magazine, 1980, 43, 979-984.	1.4	33
33	Atypically depleted upper mantle component revealed by Hf isotopes at Lucky Strike segment. Chemical Geology, 2013, 341, 128-139.	3.3	29
34	The gneiss of Zabargad Island: deep crust of a rift. Tectonophysics, 1988, 150, 209-227.	2.2	28
35	In-situ study of the eastern ridge-transform intersection of the Vema Fracture Zone. Tectonophysics, 1991, 190, 55-71.	2.2	22
36	Zabargad peridotite: Evidence for multistage metasomatism during Red Sea rifting. Geology, 1991, 19, 722.	4.4	21

CATHERINE MEVEL

#	Article	IF	CITATIONS
37	First direct observation of coseismic slip and seafloor rupture along a submarine normal fault and implications for fault slip history. Earth and Planetary Science Letters, 2016, 450, 96-107.	4.4	21
38	Pervasive silicification and hanging wall overplating along the 13°20′N oceanic detachment fault (<scp>M</scp> idâ€ <scp>A</scp> tlantic <scp>R</scp> idge). Geochemistry, Geophysics, Geosystems, 2017, 18, 2028-2053.	2.5	21
39	The MARâ€Vema Fracture Zone intersection surveyed by deep submersible Nautile. Terra Nova, 1990, 2, 68-73.	2.1	16
40	Intraoceanic tectonism on the Gorringe Bank: observations by submersible. Geological Society Special Publication, 1984, 13, 113-120.	1.3	15
41	Hydrothermal alteration studies of gabbros from Northern Central Indian Ridge and their geodynamic implications. Journal of Earth System Science, 2009, 118, 659-676.	1.3	12
42	The occurrence of deerite in highly oxidizing conditions within the ?schistes lustr�s?of eastern Corsica. Journal of Metamorphic Geology, 1986, 4, 385-399.	3.4	6
43	Occurrence and significance of gneissic amphibolites in the Vema fracture zone, equatorial Mid-Atlantic Ridge. Geological Society Special Publication, 1984, 13, 121-130.	1.3	5
44	Oceanographic Signatures and Pressure Monitoring of Seafloor Vertical Deformation in Near-coastal, Shallow Water Areas: A Case Study from Santorini Caldera. Marine Geodesy, 2016, 39, 401-421.	2.0	5
45	Fluid Circulation Along an Oceanic Detachment Fault: Insights From Fluid Inclusions in Silicified Brecciated Fault Rocks (Midâ€Atlantic Ridge at 13°20′N). Geochemistry, Geophysics, Geosystems, 2021, 22, .	. 2.5	5
46	Deerite in highly oxidizing conditions: a reply. Journal of Metamorphic Geology, 1987, 5, 557-560.	3.4	0
47	Inception and demise of a Neoproterozoic ocean basin: evidence from the Ougda complex, western Hoggar (Algeria). Geologische Rundschau: Zeitschrift Fur Allgemeine Geologie, 1996, 85, 619-631.	1.3	0